ChemComm

Accepted Manuscript

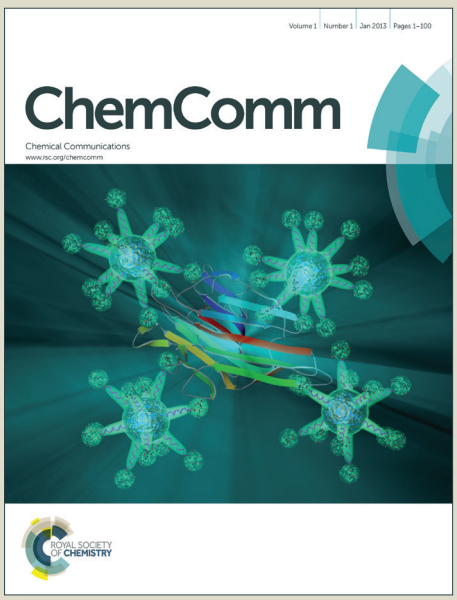

ROYAL SOCIETY OF CHEMISTRY

www.rsc.org/chemcomm

Journal Name

COMMUNICATION

Excellent Optical and Interfacial Performance of a PEDOT-*b*-PEG Block Copolymer Counter Electrode for Polymer Electrolyte-based Solid-state Dye-sensitized Solar Cells†

Received 00th January 20xx,
Accepted 00th January 20xx

DOI: 10.1039/x0xx00000x

www.rsc.org/

Tea-Yon Kim,‡[a] Wei Wei,‡[a] Woohyung Cho,[a] Sungjin Lee,[a] Jongok Won[b] and Yong Soo Kang*[a]

Poly(3,4-ethylenedioxythiophene)-*b*-poly(ethylene glycol) (PEDOT-*b*-PEG) block copolymer doped with perchlorate on FTO shows excellent optical and interfacial performance as a counter electrode (CE), such as low charge transfer resistance and low reflectivity for polymer electrolyte-based solid-state dye-sensitized solar cells (DSCs), resulting in 8.45% energy conversion efficiency, greater than common Pt CE, via a facile room-temperature process.

Dye-sensitized solar cells (DSCs) are one of the most promising alternative colorful and flexible third-generation solar cells due to their mild fabrication process, low-cost production, and applicability for large-scale fabrication.[1-3] The highest energy conversion efficiency (ECE) in such cells was recorded as 13% with a porphyrin dye and a liquid state electrolyte under 1 sun conditions.[4] DSCs are commonly composed of a dye-sensitized mesoporous semiconductor, a liquid-state electrolyte, and a counter electrode.[5] In the case of the I_3^-/ I^- redox couple, the counter electrode (CE) reduces the triiodide to monoiodide by reacting with electrons from external circuits (I_3^- + 2e- → $3I^-$).[6] Therefore, the material requires high catalytic activity, conductivity, and physical/chemical compatibility with the electrolyte.

To date, platinum (Pt) has satisfied the above requirements and has been frequently used as a CE material. However, it is rather expensive for wide application in DSCs and is also corrosive to the iodide redox couple. Therefore, a large body of alternative materials for Pt-free CE has been developed, such as carbon materials, transition metal compounds, and conducting polymers, as well as their hybrids.[7,8] Conducting polymers are particularly attractive as a Pt-free CE material because of their catalytic and conducting properties, competitive price, low-temperature processing, and easy integration into flexible devices.[9] Among these materials, poly(3,4-ethylenedioxythiophene) (PEDOT) is highlighted for its high electrical conductivity, good catalytic properties for I_3^- reduction, and remarkable stability as the CE in DSCs.[10] Additionally, PEDOT CEs have shown competitive or even better performance in comparison to Pt CEs.[7] One-dimensional (1D) nanostructured PEDOT CEs (nanotubes and nanofibers) have demonstrated outstanding performance for efficient charge transport.[11,12] PEDOT nanofibers (PEDOT NFs) produced an ECE of 9.2% with the I^-/I_3^- redox couple primarily because of the highly porous network structure.[12]

Solvent leakage and evaporation issues of liquid electrolyte result in poor long-term stability and limitations of DSC commercialization, which have motivated the development of alternative electrolytes with high stability.[13,14] Solid-state polymer electrolytes (SPEs) are attractive alternatives for device commercialization, particularly flexible DSCs, which require strong durability and good mechanical flexibility.[15,16] Even though SPE has exhibited lower photovoltaic performance than common liquid electrolytes, primarily due to its incomplete pore penetration through mesoporous TiO_2 and low ionic conductivity,[17] various efforts to complement these have been attempted.[18,19] For instance, an ECE of 8.9% for solid-state DSCs employing an SPE and Pt CE at 1 sun conditions was recently reported using the I^-/I_3^- redox couple.[20] Therefore, it would be very interesting to substitute Pt CE with PEDOT CE for solid-state DSCs employing a polymer electrolyte. In this case, compatibility between PEDOT CE and SPE will be a very crucial factor for improving ECE, where the SPE is mostly based on poly(ethylene oxide) (PEO) and its derivatives. However, even the few studies that have been reported on this issue have shown lower ECE or poorer performance than the reference data.[21-23]

[a]*Department of Energy Engineering and Center for Next-Generation Dye-Sensitized Solar Cells, Hanyang University, Seoul 133-791, Korea*
[b]*Department of Chemistry, Sejong Polymer Research Center, Sejong University, 209, Neungdong-ro, Gwangjin-gu, Seoul 143-747, Korea*
E-mail: kangys@hanyang.ac.kr
† Electronic Supplementary Information (ESI) available
‡ These authors contributed equally to this work

In this study, a new counter electrode consisting of poly(3,4-ethylenedioxythiophene)-*g*-poly(ethylene glycol) block copolymer (PEDOT-*b*-PEG) cast on a FTO glass was developed for solid state DSCs employing a PEO-based SPE using a facile fabrication process

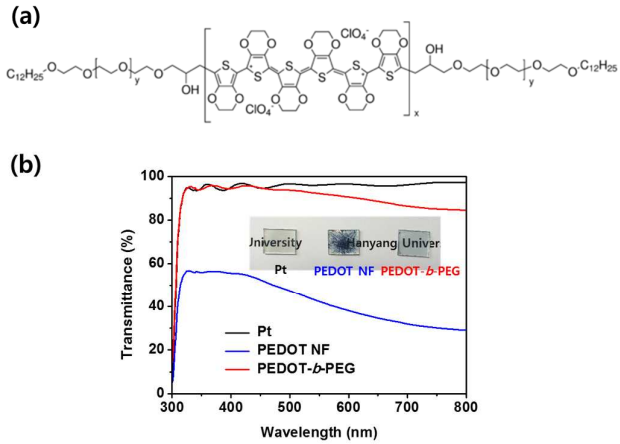

at room temperature. This CE displayed excellent optical properties, such as high transparency and low reflectivity, and surprisingly good interfacial performance with SPE of lower charge transfer resistance, compared to PEDOT NF and even Pt. The resulting ECE of DSC employing an SPE with PEDOT-*b*-PEG CE was 8.45%, which was slightly higher than that of Pt CE (8.25%), while the ECE of PEDOT NF CE was 7.83%. To the best of our knowledge, this is the highest ECE with Pt-free CE for the I^-/I_3^- redox couple and a PEO-based SPE under 1 sun conditions (AM 1.5G, 100 mW/cm^2).

Fig. 1 (a) Chemical structure of PEDOT-*b*-PEG block copolymer. (b) Optical transmittance UV-visible spectra of Pt (black-line), PEDOT NF (blue-line), and PEDOT-*b*-PEG block copolymer (red-line) coated CEs. The inset shows a photograph of each film spin-coated onto the FTO substrate.

PEDOT-*b*-PEG CE was fabricated by spin coating a 1 wt% PEDOT-*b*-PEG solution doped with perchlorate in nitromethane on FTO (Pilkington, TEC-7) at 5500 rpm (Sigma Aldrich). The chemical structure of PEDOT-PEG is shown in Fig. 1a. PEG blocks in PEDOT-*b*-PEG function as a hydrophilic adhesive to attach the hydrophobic PEDOT to the FTO substrate and increase the compatibility with the PEO-based polymer electrolyte. Therefore, the PEDOT-*b*-PEG block copolymer can make good contact with both FTO and SPE. Additionally, unlike the conventional fabrication method of Pt CE requiring a high sintering temperature (450 ℃, 30 min), PEDOT-*b*-PEG CE can be formed by evaporating the solvent at room temperature. It is very simple, in comparison even with the fabrication conditions of PEDOT NF CE (drying in a vacuum oven at 60 ℃, 2 h). This facile fabrication process of room-temperature evaporation of the PEDOT-*b*-PEG solution can also be readily applied to flexible optoelectronic devices.

Figure 1b shows another interesting character of PEDOT-*b*-PEG CE; high transparency. Even though the optical transmittance measured from the UV-visible spectra of PEDOT-*b*-PEG (red) CE is nearly equivalent with that of the Pt CE (black) at short wavelengths, it continually decreased from 450 to 800 nm and reached 82% at a wavelength of 800 nm. An optical transmittance greater than 80% in the whole visible light range is considered outstanding optical function for a CE.[24] After spin-coating with the PEDOT-*b*-PEG solution, the FTO glass changed to a light blue color but maintained high optical transparency in the complete visible region. However, PEDOT NF CE (blue) showed much lower transparency than the others. The optical transparency of PEDOT-*b*-PEG CE is also illustrated in the inset photograph in Fig. 1b. This highly transparent character of PEDOT-*b*-PEG CE originated primarily from the thickness of the PEDOT-*b*-PEG layer on the FTO. The scanning electron microscopy (SEM) images show a cross-sectional view

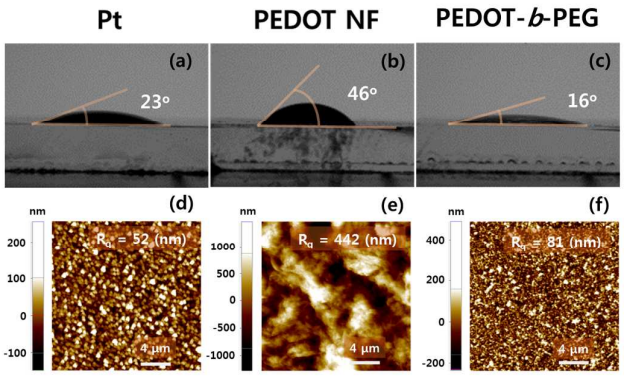

demonstrating a 50-nm thin PEDOT-*b*-PEG film coated on FTO (Fig. S1†). This high transparency of PEDOT-*b*-PEG CE can provide added value for many useful applications of DSCs such as building and vehicle windows or other installations.[25,26] The reflectance spectra were also measured in order to determine the optical character of CEs (Fig. S2†). Interestingly, except at wavelengths shorter than 400 nm, PEDOT-*b*-PEG CE showed the lowest reflectivity. This low reflectivity of PEDOT-*b*-PEG CE can also be used for bifacial DSCs (which can collect light from two sides) and even for back-side illumination conditions.[26,27]

Fig. 2 Contact angles of liquid PEG and AFM topographic images of (a) (d) Pt, (b) (e) PEDOT NF, and (c) (f) PEDOT-*b*-PEG block copolymer coated on FTO substrates. Polyethylene glycol (PEG, Mw: 400) was used as the solvent in the measurements.

To compare the suitability of the proposed CE with a PEO-based polymer electrolyte, contact angles were measured with polyethylene glycol (PEG, Mw: 400) droplets, and atomic force microscopy (AFM) images were obtained to analyze the surface properties of the fabricated CE using Pt, PEDOT NF, and PEDOT-*b*-PEG (Fig. 2). PEDOT-*b*-PEG shows a smaller contact angle (16^o) with the PEG droplet than the other samples (Pt: 23^o, PEDOT NF: 46^o). Even though PEDOT chain in PEDOT-*b*-PEG is not compatible with PEG, PEG blocks dominated the surface, resulting in the best wetting or highest compatibility with PEG (Fig. 2c). This illustrates the good compatibility between PEDOT-*b*-PEG CE and the PEO-based polymer electrolyte. For PEDOT NF, despite the large surface area and roughness (characterized by root mean square roughness, Rq) (Fig. 2e), the poor wetting property (as indicated in Fig. 2e) and the hydrophobic behavior of the PEDOT backbone enhanced the surface tension with respect to PEG (Fig. 2b). Alternatively, Rq of

PEDOT-*b*-PEG CE (81 nm) in the AFM topographic image (Fig. 2f) is greater than that of Pt CE (52 nm, Fig. 2d). This higher Rq could represent larger interfacial contact area for the improvement in the catalytic activity.

Figure 3a compares the *J-V* characteristics of C106 dye-sensitized solar cells with Pt, PEDOT NF, and PEDOT-*b*-PEG CEs, and their corresponding photovoltaic parameters are summarized in Table 1. DSCs with PEDOT-*b*-PEG CE yielded an outstanding short-circuit current density (J_{sc}) and an ECE of 8.45%. To the best of our knowledge, this ECE is the highest recorded for the I^-/I_3^- redox couple and a solid polymer electrolyte with a Pt-free CE under a 1 sun condition. However, DSCs equipped with Pt and PEDOT NF CEs showed comparatively lower J_{sc} and ECE values than those with PEDOT-*b*-PEG CE.

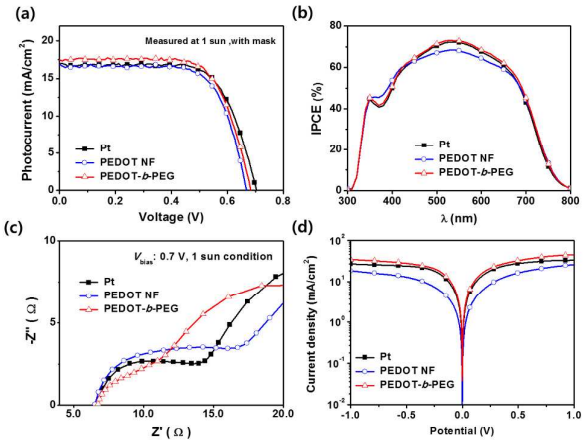

Fig. 3 (a) J-V characteristics and (b) IPCE of DSCs with Pt (black-squares), PEDOT NF (blue-circles), and PEDOT-*b*-PEG block copolymer (red-triangles) coated CEs under 1 sun illumination conditions (AM 1.5, 100 mW/cm^2 solar illumination) with a 0.21 cm^2 active area. (c) Nyquist plots at 0.7 V according to IS measurements. (d) Tafel polarization curves of symmetric cells with different CEs.

PEDOT-*b*-PEG CE also showed a higher fill factor (*FF*, 0.71) than the others (0.69), which could manifest good wetting behavior between the PEO-based polymer electrolyte and the PEDOT-*b*-PEG CE. Detailed analysis of the *FF* will be discussed later. Importantly, J_{sc} was increased in the order of PEDOT NF (16.89 mA/cm^2) < Pt (16.93 mA/cm^2) < PEDOT-*b*-PEG (17.47 mA/cm^2), and the ECE increased in the same order. Incident photon-to-electron conversion efficiency (IPCE) spectra (Fig. 3b) are in accordance with the J_{sc} tendency. Even though PEDOT-*b*-PEG CE demonstrated a smaller optical reflectance than Pt and PEDOT NF CEs (Fig. S2†), it exhibited the highest J_{sc}. Moreover PEDOT-*b*-PEG CEs employed DSCs shows the good long-term stability up to 240 hrs stored in the dart at 60 ℃ (Fig. S3†).

	V_{oc} (V)	J_{sc} (mA/cm²)	*FF*	Eff. (%)	R_{ct_T} (Ω cm²)
Pt	0.70	16.93	0.69	8.25	11.91
PEDOT NF	0.67	16.89	0.69	7.83	29.42
PEDOT-*b*-PEG	0.68	17.47	0.71	8.45	10.24

Table 1 Photovoltaic characteristics of DSCs with Pt, PEDOT NF, and PEDOT-*b*-PEG block copolymer CEs, and charge transfer resistance (R_{ct_T}) calculated using the exchange current density of Tafel plots.

Tafel polarization curves (Fig. 3d) from symmetric cells with the polymer electrolyte were obtained to evaluate the charge transfer resistance of the CEs.[28] The extrapolated intercepts of the anodic or cathodic branches in the Tafel curves indicate the exchange current density (J_0), which is directly related to the charge transfer resistance of the counter electrode.[29] In Fig. 3d, PEDOT-*b*-PEG CE shows the highest J_0, indicating better electrocatalytic activity than other CEs. Using J_0, the charge transfer resistance (R_{ct_T}) between CE and electrolyte can be calculated,[30] as listed in Table 1. These results are in good agreement with the Nyquist plot tendency measured using DSCs devices (Fig. 3c). Consequently, from the electrochemical analysis, PEDOT-*b*-PEG CE has a lower charge transfer resistance than Pt and PEDOT NF CEs, which is very consistent with the order of J_{sc}.

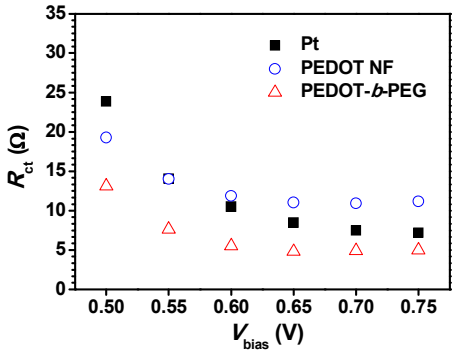

Fig. 4 Charge transfer resistance (R_{ct}) between CE and solid polymer electrolyte with respect to various bias voltages (V_{bias}) by varying CEs for DSCs estimated from the IS data at 1 sun conditions.

FF is also a very important photovoltaic parameter, which directly affects the performance of the DSCs. A bad CE increases the total series resistance (R_{series}) in DSCs, which causes an increase in overpotential and consequently decreases *FF*.[31] The R_{series} is composed of three parameters as:[6,11]

$$R_{series} = R_s + R_{ct} + R_d \quad (1)$$

Here, R_s is the sheet resistance of CE, R_{ct} is its charge transfer resistance, and R_d is the diffusion resistance through the electrolyte.

Because the same electrolyte is used for the three different CEs in this work, R_d effects can be ignored when comparing R_{series}. The three CEs showed nearly the same R_s value, based on impedance spectroscopy (IS) at various bias voltage (Fig. S4a†), regardless of the polymer layer used for CE. The bias voltage range is designed not to be flat (Fig. 3(a)) where R_{series} affects *FF*.[11] Nearly the same R_s value could be due to the fact that a thin, good attachment of the

polymer layers might complement the additional layer resistance on FTO.[6]

The charge transfer resistance R_{ct} was also estimated and plotted as a function of the bias voltage as shown in Fig. 4 with Pt (black squares), PEDOT NF (blue circles), and PEDOT-*b*-PEG (red triangles) CEs voltages under 1 sun illumination conditions. The R_{ct} value of PEDOT-*b*-PEG CE was smaller than those of the other CEs, suggesting that the PEDOT-*b*-PEG layer has better electrocatalytic activity with I_3^-, which verifies the Tafel curves shown in Fig. 3c. The other reason for a lower R_{ct} with PEDOT-*b*-PEG CE is the excellent interfacial compatibility with the PEO/PEGDME polymer electrolyte, as previously shown in Fig. 2. Thus, PEDOT-*b*-PEG CE shows a lower R_{series} (R_s+R_{ct}) than the others as shown in Fig S4b†, thus producing the highest *FF*. These results are in a good agreement with R_{ct_T} obtained from the Tafel plots and summarized in Table 1. Therefore, PEDOT-*b*-PEG is a good candidate as a new CE material for a PEO-based polymer electrolyte in the effort to achieve high device performance.

In summary, PEDOT-*b*-PEG CE yielded an ECE of 8.45% for DSCs, which is greater than those with PEDOT NF and Pt CEs (8.25%). Such high photovoltaic performance with PEDOT-*b*-PEG CE is primarily based on high J_{sc} and *FF* values due to the low charge transfer resistance between PEDOT-*b*-PEG and PEO of the polymer electrolyte, in addition to its excellent transparency and low reflectance. The low charge transfer resistance is, in turn, associated with outstanding electrocatalytic activity of PEDOT-*b*-PEG and its compatibility with PEO of the polymer electrolyte. In addition, the facile fabrication process of PEDOT-*b*-PEG CE, along with its remarkable performance with polymer electrolyte, has great potential for roll-to-roll production of flexible DSCs.

This work was financially supported by the Korea Center for Artificial Photosynthesis (KCAP) (Number 2009-0093883).

Notes and references

1. B. O'Regan and M. Grätzel, *Nature,* 1991, **353**, 737.
2. M. Grätzel, *Nature*, 2001, **414**, 338.
3. S. Ahmad, E. Guillen, L. Kavan, M. Grätzel and M. K. Nazeeruddin, *Energy Environ. Sci.*, 2013, **6**, 3439.
4. S. Mathew, A. Yella, P. Gao, R. Humphry-Baker, B. F. E. Curchod, N. Ashari-Astani, I. Tavernelli, U. Rothlisberger, M. K. Nazeeruddin and M. Grätzel, *Nat. Chem.*, 2014, **6**, 242.
5. A. Hagfeldt, G. Boschloo, L. Sun, L. Kloo and H. Pettersson, *Chem. Rev.*, 2010, **110**, 6595.
6. J. Halme, P. Vahermaa, K. Miettunen and P. Lund, *Adv. Mater.*, 2010, **22**, E210.
7. S. Yun, A. Hagfeldt and T. Ma, *Adv. Mater.*, 2014, **26**, 6210.
8. F. Hao, P. Dong, Q. Luo, J. Li, J. Lou and H. Lin, *Energy Environ. Sci.,* 2013, **6**, 2003.
9. S. Thomas, T. G. Deepak, G. S. Anjusree, T. A. Arun, S. V. Nair and A. S. Nair, *J. Mater. Chem. A,* 2014, **2**, 4474.
10. K. Saranya, Md. Rameez and A. Subramania, *Eur. Polym. J.*, 2015, **66**, 207.
11. R. Trevisan, M. Döbbelin, P. P. Boix, E. M. Barea, R. Tene-Zaera, I. Mora-Seró and J. Bisquert, *Adv. Energy Mater.*, 2011, **1**, 781.
12. T. H. Lee, K. Do, Y. W. Lee, S. S. Jeon, C. Kim, J. Ko and S. S. Im, *J. Mater. Chem.*, 2012, **22**, 21624.
13. P. Wang, S. M. Zakeeruddin, J. E. Moser, M. K. Nazeeruddin, T. Sekiguchi and M. Grätzel, *Nat. Mater.*, 2003, **2**, 402.
14. Y. Bai, Y. Cao, J. Zhang, M. Wang, R. Li, P. Wang, S. M. Zakeeruddin and M. Grätzel, *Nat. Mater.*, 2008, **7**, 626.
15. A. F. Nogueira, C. Longo and M.-A. De Paoli, *Coordin. Chem. Rev.*, 2004, **248**, 1455.
16. J. Wu, Z. Lan, J. Lin, M. Huang, Y. Huang, L. Fan and G. Luo, *Chem. Rev.*, 2015, **115**, 2136.
17. D. Song, W. Cho, J. H. Lee and Y. S. Kang, *J. Phys. Chem. Lett.*, 2014, **5**, 1249.
18. M.-S. Kang, J. H. Kim, J. Won and Y. S. Kang, *J. Phys. Chem. C*, 2007, **111**, 5222.
19. H. Chae, D. Song, Y.-G. Lee, T. Son, W. Cho, Y. B. Pyun, T.-Y. Kim, J. H. Lee, F. Fabregat-Santiago, J. Bisquert and Y. S. Kang, *J. Phys. Chem. C*, 2014, **118**, 16510.
20. W. Cho, Y. R. Kim, D. Song, H. W. Choi and Y. S. Kang, *J. Mater. Chem. A,* 2014, **2**, 17746.
21. N. Jeon, D. K. Hwang, Y. S. Kang, S. S. Im and D.-W. Kim, *Electrochem. Commun.*, 2013, **34**, 1.
22. S. Nagarajan, P. Sudhagar, V. Raman, W. Cho, K. S. Dhathathreyan and Y. S. Kang, *J. Mater. Chem. A,* 2013, **1**, 1048.
23. S. Y. Heo, J. K. Koh, J. K. Kim, C. S. Lee and J. H. Kim, *Electrochim. Acta,* 2014, **137**, 34.
24. J. E. Trancik, S. C. Barton and J. Hone, *Nano Lett.*, 2008, **8**, 982.
25. F. Gong, H. Wang, X. Xu, G. Zhou and Z.-S. Wang, *J. Am. Chem. Soc.*, 2012, **134**, 10953.
26. Q. Tai and X.-Z. Zhao, *J. Mater. Chem. A,* 2014, **2**, 13207.
27. Y. Duan, Q. Tang, J. Liu, B. He and L. Yu, *Angew. Chem. Int. Ed.*, 2014, **53**, 14569.
28. M. Wang, A. M. Anghel, B. Marsan, N.-L. C. Ha, N. Pootrakulchote, S. M. Zakeeruddin and M. Grätzel, *J. Am. Chem. Soc.*, 2009, **131**, 15976.
29. I. Hwang and K. Yong, *ChemElectroChem*, 2015, **2**, 634.
30. F. Liu, J. Zhu, Y. Xu, L. Zhou, Y. Li, L. Hu, J. Yao and S. Dai, *Chem. Commun.*, 2015, **51**, 8108.
31. G. Hodes, *J. Phys. Chem. Lett.,* 2012, **3**, 1208.